

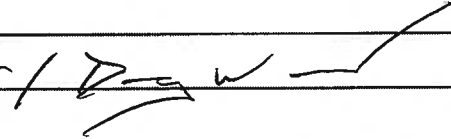
APPENDIX E

FCT DOCUMENT COVER SHEET ¹

Name/Title of Deliverable/Milestone/Revision No. Status Report on Radionuclide Solubility Experimental Studies/ M3FT-13LA08180111

Work Package Title and Number DR Salt R&D - LANL FT-13LA081801

Work Package WBS Number 1.02.08.18

Responsible Work Package Manager Doug Weaver / 
(Name/Signature)

Date Submitted

Quality Rigor Level for Deliverable/Milestone ²	<input checked="" type="checkbox"/> QRL-3	<input type="checkbox"/> QRL-2	<input type="checkbox"/> QRL-1 <input type="checkbox"/> Nuclear Data	<input type="checkbox"/> Lab/Participant QA Program (no additional FCT QA requirements)
--	---	--------------------------------	---	---

This deliverable was prepared in accordance with Los Alamos National Laboratory
(Participant/National Laboratory Name)

QA program which meets the requirements of
 DOE Order 414.1 NQA-1-2000 Other

This Deliverable was subjected to:

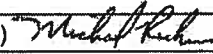
Technical Review

Technical Review (TR)

Review Documentation Provided

- Signed TR Report or,
- Signed TR Concurrence Sheet or,
- Signature of TR Reviewer(s) below

Name and Signature of Reviewers

Michael K. Richmann (LANL)  9/30/13

Peer Review

Peer Review (PR)

Review Documentation Provided

- Signed PR Report or,
- Signed PR Concurrence Sheet or,
- Signature of PR Reviewer(s) below

NOTE 1: Appendix E should be filled out and submitted with the deliverable. Or, if the PICS:NE system permits, completely enter all applicable information in the PICS:NE Deliverable Form. The requirement is to ensure that all applicable information is entered either in the PICS:NE system or by using the FCT Document Cover Sheet.

NOTE 2: In some cases there may be a milestone where an item is being fabricated, maintenance is being performed on a facility, or a document is being issued through a formal document control process where it specifically calls out a formal review of the document. In these cases, documentation (e.g., inspection report, maintenance request, work planning package documentation or the documented review of the issued document through the document control process) of the completion of the activity, along with the Document Cover Sheet, is sufficient to demonstrate achieving the milestone. If QRL 1, 2, or 3 is not assigned, then the Lab / Participant QA Program (no additional FCT QA requirements) box must be checked, and the work is understood to be performed and any deliverable developed in conformance with the respective National Laboratory / Participant, DOE or NNSA-approved QA Program.



**Status Report on Radionuclide Solubility
Experimental Studies
M3FT-13LA08180111**

9/30/13

**Prepared for the U.S. Department of Energy
Used Fuel Disposition Campaign**

**Donald T. Reed
Michael Dugas, Julie Swanson and Amelia Hayes**

**Actinide Chemistry and Repository Science Program
Repository Science and Operations
Los Alamos National Laboratory**

LA-UR 13-27644

Executive Summary

An understanding of the relevant actinide and brine chemistry is a critical need for the safety case for a salt-based nuclear repository. Although a salt repository is predicted to be dry during its performance lifetime, there are low-probability brine-inundation scenarios, mostly due to human intrusion, that must be considered in the regulatory licensing process. This need is best exemplified by the ongoing recertification effort in the Waste Isolation Pilot Plant (WIPP), and the FEPs associated with this project, where brine and actinide chemistry is shown to be a critical part of the safety case.

In this project, we proposed to start the process of extending actinide brine chemistry studies to the higher temperatures that are predicted for the disposal of HLW/SF in a salt-based repository. Although some modeling predictions exist, it is important to directly measure and establish the effects of temperature on the solubility of key actinides important to release, the effects of redox processes that determine their oxidation state, and associated processes (e.g., radiolysis and microbial effects) that can influence this chemistry. This project scope had to be greatly reduced due to funding limitations and was refocused on a general assessment of the actinide science needed and a specific focus on the biogeochemistry of neptunium (V) to begin the evaluation of thermal effects. Progress in this area is reported in this final report with the following key features/results:

- An overall assessment of the current state and data needs was completed and provided to the DOE as an overall basis for the actinide work.
- Progress is reported on two important supporting aspects of the broader proposed study: Extended iron analysis and the solubility of Fe(II) in high magnesium brine systems; and the evaluation of techniques for the measurement of water in salt.
- A detailed study on the effects of ionic strength and temperature on Np(V) aquo species was completed. Spectral features were characterized. This is fundamental to continued studies of the aqueous chemistry of Np(V) in brine and these results are the basis of a publication that is in preparation.
- The complexation borate with Np(V) was investigated as an example complex of Np(V) that is specific to salt-based brine chemistry. The room temperature study as a function of ionic strength was completed. This work is also the basis of a publication that is in preparation.
- Microbial studies were extended in two ways. The microbial characterization of Gorleben salt was initiated. Additionally, the bio-association of Np(V) with a representative archaea (*Halobacterium noricense*) was investigated. This research is also part of a manuscript that is in preparation for publication and these are the first results for the biosorption of actinides with archaea.

There remains a long way to go to fully address the issue of actinide behavior in a thermal salt-based repository. The benefit of these initial results to the DOE is that fundamental scientific results were obtained that start this process for the Np(V) system, which is a key actinide and oxidation state for the long-term safety case.

TABLE OF CONTENTS

Section	Page
1.0 Summary of Key Accomplishments	4
2.0 Assessment of Research Needs for Actinide and Brine Chemistry in Support of an HLW/SF Repository in Salt	6
2.1 Data Need and Gaps in Actinide Brine Chemistry	6
2.2 International Collaboration and Programs	9
3.0 Status of Experimental Results: Developmental of Expanded Analytical Capability in Salt/Brine Systems	10
3.1 Iron (II) Analysis and Solubility in Brine	10
3.1.1 Modified Ferrozine® Method	10
3.1.2 Solubility of Fe(II) in MgCl ₂ Brine	13
3.2 Measurement of Water Content in Salt	15
3.2.1 Gravimetric Analysis	15
3.2.2 Coulometric Analysis (Karl-Fischer)	17
3.2.3 Use of Microcalorimetry for the Analysis of Water in Salt	18
3.2.4 Overall Status and Assessment of Techniques	21
4.0 Status of Experimental Results: Biogeochemistry of Neptunium (V)	23
4.1 Task 3: Microbial Characterization of Gorleben Salt and Biosorption	23
4.2 Task 4: High Ionic-Strength and Temperature Effects on the Np(V) Aquo species	27
4.3 Task 5: Np(V) Borate Complexation	31

Status Report on Radionuclide Solubility Experimental Studies M3FT-13LA08180111

9/30/13

The speciation, solubility, oxidation-state distribution and consequently the potential mobility of multivalent actinides in a high-level waste (HLW/SF) salt-based nuclear repository remains a key consideration in defining the overall performance of a permanent geologic repository. Multivalent actinides of primary importance are americium, plutonium, neptunium and uranium. An assessment of the chemistry of these key HLW/SF constituents under the range of conditions in a potential HLW/SF repository is needed to define the radionuclide source term that is likely needed to evaluate overall repository performance.

In this project, we proposed to start the process of extending actinide brine chemistry studies to the higher temperatures that are predicted for the disposal of HLW/SF in a salt-based repository. Although some modeling predictions exist, it is important to directly measure and establish the effects of temperature on the solubility of key actinides important to release, the effects of redox processes that determine their oxidation state, and associated processes (e.g., radiolysis and microbial effects) that can influence this chemistry. This project scope had to be greatly reduced due to funding limitations and was refocused on a general assessment of the actinide science needed and a specific focus on the biogeochemistry of neptunium (V) to begin the evaluation of thermal processes. Progress in this area is summarized in this final report

1.0 Summary of key Accomplishments

Key progress/accomplishments in the actinide science activity are:

- An overall assessment of the current state and data needs was completed and provided to the DOE as an overall basis for the actinide work. Two reports were provided:
 - Integrated Report on the Results of International Workshops (M3FT-12LA08180117)
 - Status Report on LANL International Collaboration (M4FT-12LA08180114)

- The oxidation-specific analysis of iron in brine systems at high pH was extended to increase the overall sensitivity of the Ferrozine® analysis method. Solubility studies were initiated in high magnesium chloride brines at variable pH and the status of these ongoing studies is reported. The chemistry of iron is closely linked to the actinide redox issues and its redox chemistry, as a function of temperature, critical to predicting oxidation-state distributions in brine-intrusion scenarios.
- Three techniques were evaluated for the measurement of water in salt: Gravimetric, coulometric and calorimetric. The water content of salt is important in understanding the availability of brine and its likely compositional range in a thermal salt repository. Of these, the gravimetric and coulometric are the most promising although calorimetry can give more detailed information on the associated phases if completely understood.
- A detailed study on the effects of ionic strength and temperature on Np(V) aquo species was completed. Spectral features were characterized. This is fundamental to continued studies of the aqueous chemistry of Np(V) in brine and these results are the basis of a publication that is in preparation.
- The complexation borate with Np(V) was investigated as an example complex of Np(V) that is specific to salt-based brine chemistry. The room temperature study as a function of ionic strength was completed. This work is also the basis of a publication that is in preparation.
- Progress on the microbial characterization of Gorleben salt is reported. This was done using the same protocols and techniques used in the WIPP project and are the basis of a collaboration with Rossendorf (Germany) researchers and a designated activity in the NEA salt club.
- The bio-association of Np(V) with a representative archaea (*Halobacterium noricense*) was also investigated. The archaea appear to behave very differently than bacteria and have much weaker and less pH-dependent association than bacteria under similar conditions. This research is also part of a manuscript that is in preparation for publication and these are the first results for the biosorption of actinides with archaea.

2.0 Assessment of Research Needs for Actinide and Brine Chemistry in Support of an HLW Repository in Salt

An understanding of the relevant actinide and brine chemistry is a critical need for the safety case for a salt-based nuclear repository. Although a salt repository is predicted to be dry during its performance lifetime, there are low-probability brine-inundation scenarios, mostly due to human intrusion, that must be considered in the regulatory licensing process. This need is best exemplified by the ongoing recertification effort in the Waste Isolation Pilot Plant (WIPP), and the FEPs associated with this project, where brine and actinide chemistry is shown to be a critical part of the safety case.

2.1 Data Needs and Gaps in Actinide Brine Chemistry

The goal of this task was to provide an overview assessment of where we are in the WIPP project as it relates to the data/research needs and gaps for an HLW/SF salt-based repository. In this context, this is a first step in the process of fully identifying research needs in this area and is built on a series of US-German workshops on this subject. The extension of the safety case from the WIPP TRU repository to an HLW/SF nuclear repository (defense or commercial) is relatively straightforward and many aspects of the current WIPP safety case and approach will apply. There are, however, some research and data needs that are specific to the HLW/SF case that still need to be addressed. These mainly fall into two categories: 1) research that has not been done because it does not apply to the WIPP case; 2) improvements to fill data gaps in the existing WIPP safety case to further define the conservatism in place.

The WIPP safety case has been extensively reviewed and defended to EPA which is the regulator for the WIPP repository. This safety case properly addresses the brine and actinide chemistry important for the TRU repository since there are low-probability brine intrusion scenarios that the regulator has required the WIPP project to address. In this context, many of these same arguments extend to the HLW/SF case and it is critical to address these to assure compliance should a decision go forward to license a HLW/SF repository in Salt.

There are however a number of aspects of this safety case that could be improved to remove or define conservatism and there are a number of issues that are properly ignored by the

WIPP safety case, that are important for the HLW/SF case, because they do not apply. These were described in more detail in section 2, and are summarized below:

WIPP Geology and Repository Environment

- WIPP geology and geochemical data pertain to temperature conditions at ~ 25°C. This is a clear limitation of the safety case as elevated temperatures will likely be present in an HLW/SF repository.
- The lack of a good understanding of the microbiology associated with salt formations was a critical limitation in the safety case that forced very conservative assumptions and engineering decisions that were relatively costly for the WIPP project. It is critical to develop a robust understanding of microbial effects in salt so that these effects can be accounted for in the HLW/SF safety case and, in many cases, shown to be insignificant and therefore eliminated from consideration.
- The phases found in salt are relatively well understood and are somewhat ubiquitous among the many salt formations that have been studied worldwide. The effects of temperature on the stability of these phases and their potential towards alteration are an added data need that is specific to the HLW/SF case.
- The presence of water in salt and the humidity associated with this water is well understood in the absence of thermal effects - as is the case in WIPP. The potential effect of temperature on inclusions, water availability and relative humidity are needed to understand what happens in the absence of brine intrusion and are needed inputs to predict microbial behavior.

Brine Chemistry

- The Pitzer model needs to be made more robust to fill in existing gaps in the description of magnesium and iron chemistry – two components of the repository that will likely have important impacts on the overall chemistry.
- There is little/no data on the effect of temperature on Pitzer formulations in high ionic strength systems. Selected experiments coupled with strategic extrapolation from

existing room temperature data are needed to extend the Pitzer model to the higher temperatures expected in the HLW/SF case.

Radionuclide Chemistry

- Extension of the oxidation state approach to radionuclides beyond the TRU considered extensively in the WIPP case – most importantly Tc, U, Cs, Sr and lesser fission products.
- Effect of temperature on all radionuclide solubilities. Increased temperature is expected to result in lower solubilities. This however needs to be demonstrated experimentally and supported by modeling.
- Extension of the Pitzer formations for actinide species to the higher temperatures needed for HLW/SF.
- Investigations to show that the redox mechanisms in place in the WIPP, primarily reactions with Fe, extend to the higher temperatures expected in the HLW/SF case.
- Inclusion of radiolytic effects on radionuclide solubility and oxidation state distribution. This is excluded from consideration in the WIPP due to the low background activity and overwhelming effects of the iron chemistry.
- Greater emphasis on uranium as its chemistry will affect the other radionuclides – especially for spent fuel.
- Improved oxidation state analogs for the An(IV) oxidation state. Thorium, which is the analog currently used by the WIPP, although conservatively high is a very poor analog for the An(IV) oxidation state in many respects. Using plutonium(IV), or neptunium(IV) would greatly improve the accuracy of the results and better define the conservatisms present.

2.2 International Collaboration and Programs

There are four international activities that were engaged for the international component of the radionuclide solubility NE project. These are:

- 1) A combined US-German assessment report on data and research needs for brine and actinide chemistry that includes elevated temperatures is in process and continues. This is an extension of the US-focused FY-12 report provided to DOE-NE by the Los Alamos radionuclide solubility project. A working group under the NEA salt club was established and this work now continues in this venue.
- 2) Microbial characterization research to establish the indigenous microbial population of Gorleben salt and samples from long-standing Polish salt mines is ongoing. This continues as an NEA salt club activity.
- 3) We are looking into initiating a synchrotron-based analysis project to used XAFS/XANES to characterize the oxidation state and location of first-release fission products from spent fuel. This is being developed as a contribution to the First Nuclides project and collaboration with PSI and INE researchers. This collaboration was not developed due to limitations in funding.
- 4) The planning of the Los Alamos – INE ABC Salt III workshop was held in April 2013 in Santa Fe. This was well attended and well received by the international community. A follow-up to this workshop is tentatively planned for May 2015.

3.0 Status of Experimental Results: Development of Expanded Analytical Capability in Salt/Brine Systems

Progress in the following Tasks is reported:

Task 1: Iron (II) Analysis and Solubility in Brine

Task 2: Measurement of Water Content in Salt

3.1 Task 1: Iron (II) Analysis and Solubility in Brine

Progress in two areas was made: Iron analysis and solubility in high ionic strength brines. The iron analysis was done using a modified Ferrozine® method that extended past work in this area and is needed to investigate the redox chemistry that links to actinide systems.

3.1.1 Modified Ferrozine® method

The purpose of this activity was to test and redevelop the Ferrozine® method for sensitivity in brine systems. In some of the current experiments in brine solutions, iron content cannot be analyzed by utilizing Ferrozine® due to the breakdown of Fe-Ferozine® complex in solution, causing an inaccurate reading in iron levels. A comparative study between the GeneSys 20 and the Cary 5000 spectrophotometers was also performed.

A modified version of the normal calibration curve conducted on the GeneSys 20 spectrophotometer was utilized during this phase of experimentation. Following the standard calibration method, 10µL of Fe²⁺ stock (.416M FeCl₂ in .1 M HCl) was added into 490 µL of 3.95M HCl in order to gain the iron standard used. Dilutions were taken from this standard in the following experiments. After each solution was prepared and equilibrated, 50µL of each sample was added to 202µL of .62M hydroxylamine and 248 µL of HPW. After equilibration, 100µL of the solution was added to 900µL of Ferrozine® and then analyzed with both spectrophotometers.

The results of this comparative study are presented in Figures 3.1-1 and 3.1-2. At the highest dilution, it was necessary to analyze the entire spectrum due to background elevation (CARY spectrometer data). Overall this method modification, using 10X concentrated Ferrozine® to more completely complex the Fe²⁺ and fully analyzing the spectrum using the

CARY 5000 to account for background elevation gave an effective 100X increase in sensitivity that is critical to the analysis of reduced iron in brine systems and allowed for the analysis of the iron oxidation state in the solubility studies completed.

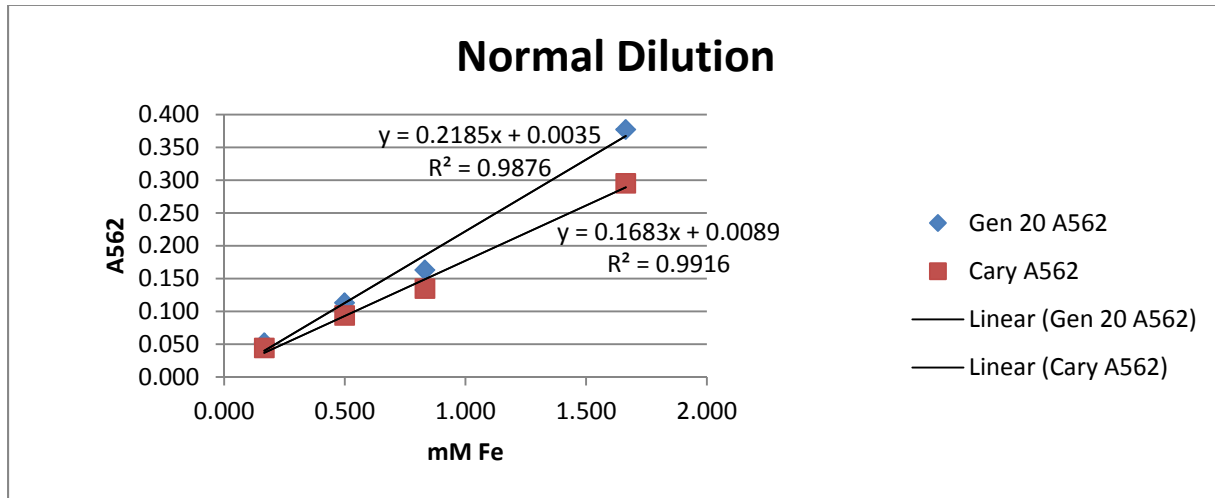


Figure 3.1-1 Comparison of the OD response on the CARY 5000 vs. Gen 20 spectrometers for the usual Ferrozine® procedure. Linear response was only observed in the CARY instrument with high scatter contributing to a falsely high response for the GEN 20 spectrometer.

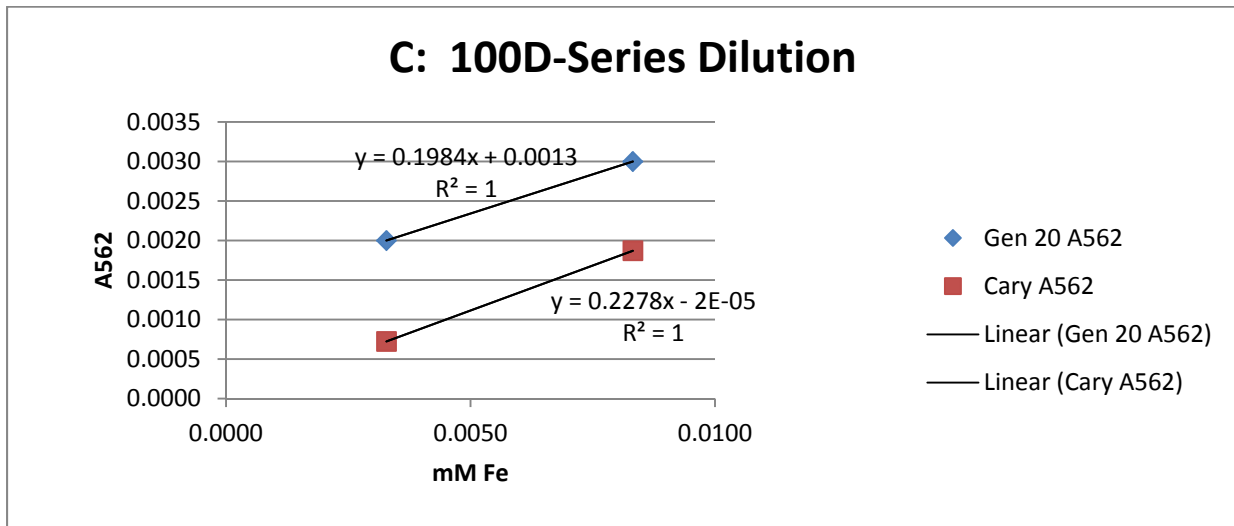
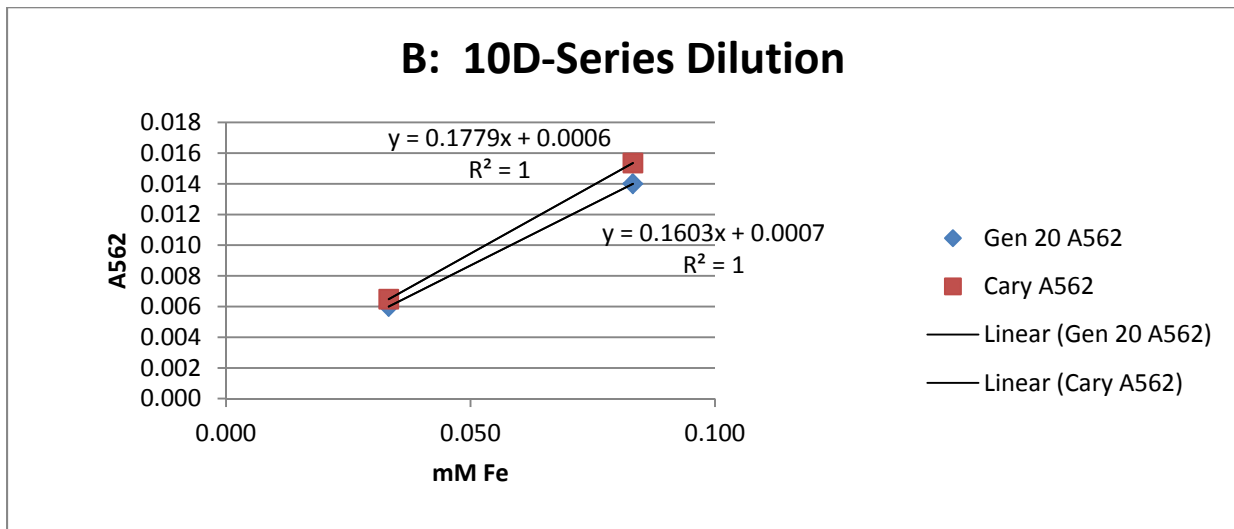
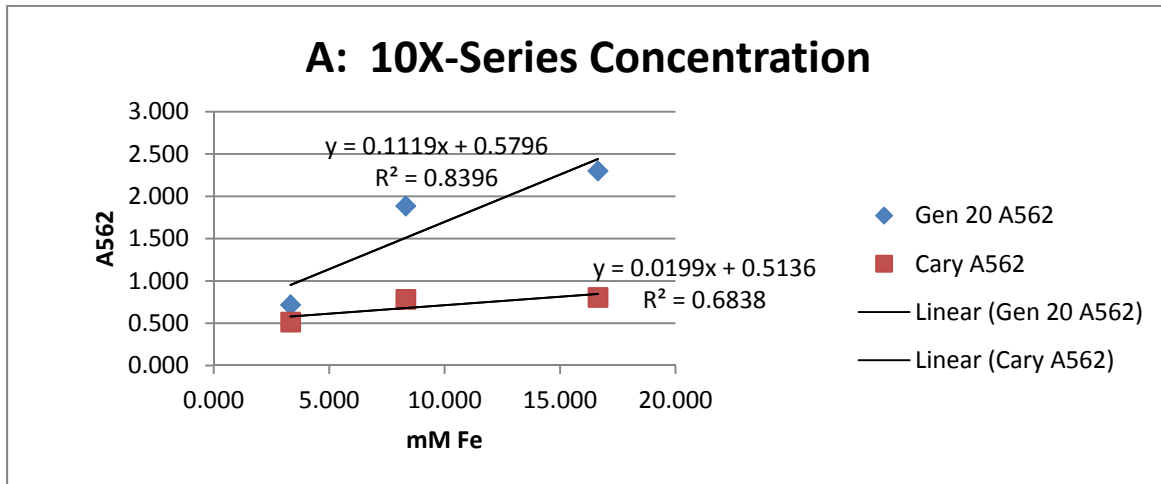


Figure 3.1-2 OD comparison for 10X concentration(a), 10D dilution(b) and 100D dilution(c).

3.1.2 Iron(II) Solubility in Magnesium Chloride

A number of past experiments we have conducted show that we have sparingly soluble Fe^{2+} at moderately high pH, although the solubility can be quite high at low pH (<6). Since reduced iron (Fe^{2+}) is a key reductant of higher-valent actinides, it was critical to evaluate its overall solubility in brine.

A 2.3 molar magnesium chloride stock solution was prepared and degassed in order for the experiment to be carried out in a glove box for pH 4 through 9. A 9.74×10^{-3} Molar solution of magnesium chloride was prepared and degassed for pH 10 through 12. Each of the stock brines were approximately 55mL in volume. A PIPES buffer was added to the samples in the range of pH 6 through 8 to provide additional pH stability. A buffer was not added to the other brines, since these brines were not in the buffer's pH range capacity. Each brine was titrated to the given pH, and, due to the high salt concentration, was corrected to give a pC_{H^+} value used in the experiment. These were titrated using sodium hydroxide, 3.95M and 12M hydrochloric acids. Once the pH stock solutions were at the correct pC_{H^+} , 10mL samples were taken and used for the iron solubility experiments. Each sample was given an amount of iron (II) chloride tetrahydrate powder until a precipitate formed or until saturation occurred. The samples were analyzed for sodium, magnesium, and iron content using the ICP-MS and the Ferrozine® method for iron described earlier in this section and compared to ICP-MS iron analysis data.

The initial results of this study are show in Table 3.1-1. Overall the solubility of Fe(II) in solution is quite low at $\text{pH} > 8$ and well below 1 mM in concentration. These preliminary data provide a good baseline for future studies and demonstrate that the ICP-MS and Ferrozine method can work in these brine systems. Some inconsistency was however observed and this is likely due to complications between colloidal and non-colloidal contributions of Fe(II) to the analyses performed and this complexity is the subject of future work.

Table 3.1-1 Ferrozine and ICP-MS analysis of Fe (II) in Magnesium-Chloride Brine as a function of pC_{H+}

Ferozine® Data:

Sample	pH	Fe2 A562	mM Fe2	Total A562	Total mM Fe	mM Fe3	Fe Ratio	Fe 2/Total	Molarity	Average (mM)
pH 4A	4.10	0.100	1646.286	0.104	1736.866	90.580	18.175	0.948	1.646	1.680
pH 4B	4.10	0.103	1714.221	0.101	1668.931	45.290	-37.850	1.027	1.714	
pH 5A	5.10	0.103	1714.221	0.105	1759.511	45.290	37.850	0.974	1.714	1.703
pH 5B	5.10	0.102	1691.576	0.106	1782.156	90.580	18.675	0.949	1.692	
pH 6A	5.90	0.054	604.620	0.054	604.620	0.000	#DIV/0!	1.000	0.605	0.605
pH 6B	5.90	0.054	604.620	0.055	627.264	22.645	26.700	0.964	0.605	
pH 6C	5.90	0.175	334.466	0.189	366.168	31.703	10.550	0.913	0.334	0.345
pH 6D	5.90	0.184	354.846	0.184	354.846	0.000	#DIV/0!	1.000	0.355	
pH 7A	7.20	0.139	252.944	0.155	289.176	36.232	6.981	0.875	0.253	0.254
pH 7B	7.20	0.140	255.208	0.166	314.085	58.877	4.335	0.813	0.255	
pH 8A	7.80	0.107	180.480	0.113	194.067	13.587	13.283	0.930	0.180	0.182
pH 8B	7.80	0.108	182.745	0.097	157.835	24.909	-7.336	1.158	0.183	
pH 9A	8.90	0.282	65.325	0.290	67.530	2.205	29.625	0.967	0.065	0.066
pH 9B	8.90	0.284	65.877	0.281	65.050	-0.827	-79.667	1.013	0.066	
pH 10A	9.80	0.551	139.471	0.550	139.195	-0.276	-506.00	1.002	0.139	0.139
pH 10B	9.80	0.549	138.920	0.551	139.471	0.551	252.000	0.996	0.139	
pH 11A	10.90	0.621	158.765	0.630	161.246	2.481	64.000	0.985	0.159	0.159
pH 11B	10.90	0.626	160.143	0.635	162.624	2.481	64.556	0.985	0.160	
pH 12A	11.90	0.337	80.485	0.341	81.588	1.103	73.000	0.986	0.080	0.081
pH 12B	11.90	0.340	81.312	0.340	81.312	0.000	N/A	1.000	0.081	

ICP-MS Analysis

Sample	pH	ICP-MS A(ppb)	ICP-MS B(ppb)	Molarity A	MolarityB	Average
Iron						
pH 4	4.1	1300	1500	1.862	2.149	2.005
pH 5	5.1	1300	1200	1.862	1.719	1.791
pH 6	5.9	1200	1400	0.430	0.501	0.466
pH 7	7.2	870	920	0.312	0.329	0.321
pH 8	7.8	560	500	0.201	0.179	0.190
pH 9	8.9	220	230	0.079	0.082	0.081
pH 10	9.8	480	610	0.172	0.218	0.195
pH 11	10.9	910	590	0.326	0.211	0.269
pH 12	11.9	330	320	0.118	0.115	0.116

3.2 Measurement of Water Content in Salt

An evaluation of gravimetric, coulometric, and calorimetric methods for the detection of water in salt was performed. This is needed to establish brine availability and benchmark the planned variable-temperature brine chemistry actinide studies.

A weight loss determination and Karl Fischer titration was performed to determine water content using salt sample SDI-SMP-00037, which was collected from N940 & E1200 at WIPP. Calorimetry was also considered. The different methods were compared to evaluate their potential for water analysis in salt. These studies focused on sample SDI-SMP-00037 which was taken from a debris pile in the WIPP and was considered ideal for this first test because it contains mainly halite with minimal clay minerals and was obtained from the likely area for SDDI experiments and test.

3.2.1 Gravimetric (weight loss) Method

One piece of sample SDI-SMP-00037 was broken into fragments that were separated into three subsamples. These subsamples were designated SDI-SMP-00037.1, which contains a moderate amount of material previously exposed to air; SDI-SMP-00037.2, which contains only a minimal amount of material from the surface of the original sample; and SDI-SMP-00037.3, which contained the highest amount of material previously exposed. The samples were weighed individually before any further breakup of the fragments. Table 3.2-1 lists the masses measured.

Table 3.2-1 Initial mass measurements of the salt samples and blender			
Sample Number	Mass of Sample in Container (g)	Mass of Container (g)	Calculated Mass of Sample (g)
SDI-SMP-00037.1	272.7419	37.3613	235.3806
SDI-SMP-00037.2	211.2337	37.3145	173.9192
SDI-SMP-00037.3	274.3887	37.0560	237.3327

The samples were then ground in individual Waring blender samples cups and reweighed. Although there was a slight loss of salt in this process, and a small amount of vapor

loss could have occurred, most of the change in mass was believed to be water. For this reason, however, the calculated percent H₂O are the maximum possible values.

The samples SDI-SMP-00037.1, 2, and 3 were further separated into portions designated for the different methods. At each step the samples were weighed and the mass loss calculated. Smaller samples for titration and calorimetry were measured out and bulk samples were measured for the weight loss method.

The weight loss samples were placed in an oven at 115°C for a period of seven days. Over this time, the samples were removed from the oven to be weighed and the change in mass was calculated. The maximum total percent water was calculated by adding the percent water from sample preparation and the percent water from heating in the oven. The change in % water over time are presented in Table 3.2-2 and shown in Figure 3.2-1.

Table 3.2-2 Mass loss due to heating salt to ~ 115 °C							
Sample Number	Mass loss Whole Sample Prep (g)	% H ₂ O Whole Sample Prep	Mass loss Partial Sample Prep (g)	% H ₂ O Partial Sample Prep	Mass loss Oven Heating (g)	% H ₂ O Oven Heating	Maximum total % H ₂ O
SDI-SMP-00037.1a	0.7754	0.3294	0.0030	0.0013	0.5509	0.5315	0.8622
SDI-SMP-00037.2a	0.7032	0.4043	-0.0005	-0.0003	0.5166	0.4832	0.8872
SDI-SMP-00037.3a	1.3097	0.5518	0.0096	0.0043	0.5731	0.5441	1.1002

The results of this gravimetric approach gave good consistency with a water content value of ~ 1% which is consistent with what is frequently observed in the WIPP. Further work is needed to insure that all water is being accounted for in this approach, but this appears to be a good/reliable approach to the determination of the bulk water content in halite-dominated salt. This approach needs to be further evaluated for clay-dominated salt where greater water content and complexity is expected.

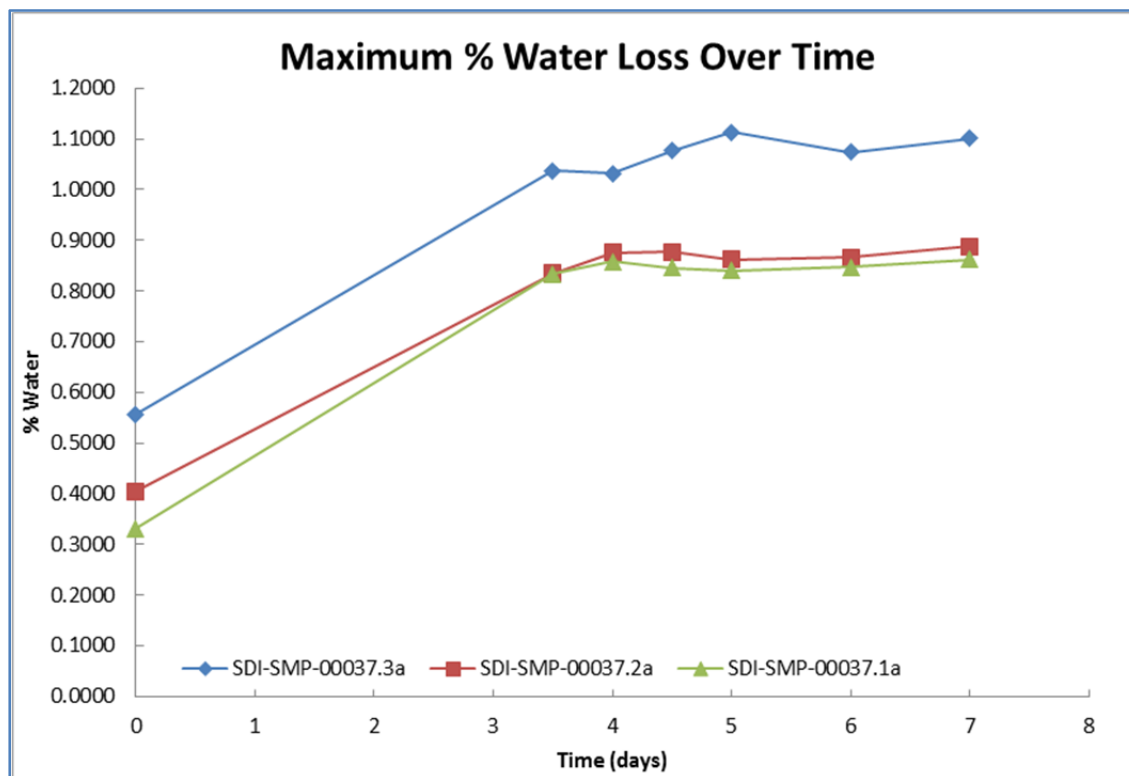


Figure 3.2-1 Observed weight loss as a function of time while heating to 115 °C

3.2.2 Coulometric Analysis (Karl Fischer Titration)

Initial results on the Karl Fischer titration approach are given in this section. Karl Fischer titrators measure the concentration of water within a sample and the salt sample, in its entirety, is destructively dissolved into an organic matrix (usually a 1:1 mixture of methanol and formamide). The coulometric Karl Fischer titrator is ideal for samples expected to have a low concentration of water (from 1 ppm to 5% for the Mettler Toledo C20X) and typically much smaller samples (~ gram size) are used. This is likely a good technique for post drying analysis of salt in planned SDDI experiments where low water contents are expected.

Samples from SDI-SMP-00037 were measured and mixed with 30 mL of solvent. The samples were shaken periodically and placed in a 50°C oven for an hour to dissolve and release as much water as possible from the halite. All of the samples added to the solvent were less than 1.0 gram, however total dissolution was not observed. Four of these samples were analyzed by Karl Fischer titration with the results presented in the chart shown in Table 32-3.

Table 3.2-3 Initial results from the Coulometric analysis for the water content in salt					
Sample	Mass of sample, syringe, and beaker (g)	Mass of syringe and beaker (g)	Mass of sample (g)	Result of titration (ppm)	Result of titration (%)
SDI-SMP-00037.1bi	113.565	111.2403	2.3247	824.9	0.082
SDI-SMP-00037.2bi	113.8979	112.1933	1.7046	1148.7	0.115
SDI-SMP-00037.2bii	113.7586	112.1809	1.5777	1257.9	0.126
SDI-SMP-00037.2biii	113.328	112.1936	1.1344	1384.3	0.138

The Karl-Fischer coulometric approach is a technique that is widely used for the trace-level detection of water in various media. The results just presented remain inconclusive for this specific application and probably exceeded the sample size that can be addressed by this technique.

3.2.3 Use of Microcalorimetry for the Analysis of Water in Salt

A TA Instruments TAM-III nanocalorimeter was installed. This device will aid in the determination of thermodynamic parameters needed to perform reaction system modeling and in particular, Pitzer parameter determinations for high ionic strength modeling. The system has 1 and 4 mL static hastelloy ampoules, as well as an accessory isothermal titration system. As such, the system will be capable of performing typical static reaction calorimetry (isothermal, solution and reaction types) with heat flow sensitivity in the nano to low-milliwatt range.

Thermodynamic parameters that are determinable include binding constant, stoichiometry, enthalpy, heat capacity, entropy and free energy. In addition, while not optimized for performing high-speed differential scanning calorimetry, this unit can do so at slower speeds (typically 2°C/hour).

Instrument Check and Calibration: Heat Capacity of Water

The determination of the heat capacity at room temperature of a reference substance was performed using high-purity water (HPW). In this case, a known amount of high purity water (252.6 mg) was used with a company supplied protocol that cycles the calorimeter upwards and downwards one degree three times around the typical value of room temperature, 25 °C. This generates three heat capacity results, which are then processed to generate a mean value with associated uncertainty. The difference between the mean and the literature heat capacity value is used to set the calorimeter gain. The result obtained was within the TA Instruments recommended error limit of $\pm 1\%$ (an error relative to the literature value of 0.62% was obtained) and no change to the gain is necessary.

The most difficult experiment, ironically, turns out to be baselining the system for titration work, since it involves all of the techniques taught by the TA Instruments trainer, as well as pushing the instrument to its limiting sensitivity. This was accomplished with the results as shown in Figure 3.2-2 and Table 3.2-4.

The heat flow plot reflects the work function of titrating water from the syringe system into a water sample in the calorimeter. Analysis of the data (see Table 3.2-4) shows an average heat flow of 71.5 ± 2.1 μJ per 10 μL water injection aliquot into a 900 μL water sample. This heat flow would be subtracted off or baselined from any titration experiment using a water-based titrant into a water-based sample using the same titration parameters and demonstrates the high degree of sensitivity of this instrument.

Table 3.2-4 Peak by peak analysis of the heat flow generated by injecting water into water.						
Section name	No. of data	Duration seconds	Mean	Slope	Integral Joules	Peak Area Joules
Initial baseline	299	300.151	-1.333E-09	-1.259E-10	-3.978E-07	
Titration 1	226	225.602	3.283E-07	-3.013E-09	7.435E-05	7.461E-05
Baseline 1	74	75.094	-9.734E-10	1.139E-09	-5.943E-08	
Titration 2	226	225.556	3.149E-07	-2.938E-09	7.130E-05	7.078E-05
Baseline 2	74	75.138	5.595E-09	-5.117E-10	4.291E-07	
Titration 3	225	224.714	3.110E-07	-2.910E-09	7.014E-05	7.029E-05
Baseline 3	74	74.880	-6.886E-09	-1.644E-10	-5.236E-07	
Titration 4	226	225.712	3.084E-07	-2.993E-09	6.986E-05	7.043E-05
Baseline 4	300	300.614	1.824E-09	-1.206E-10	5.516E-07	
					Mean (μJ) =	71.53
					Stdev (μJ) =	2.06

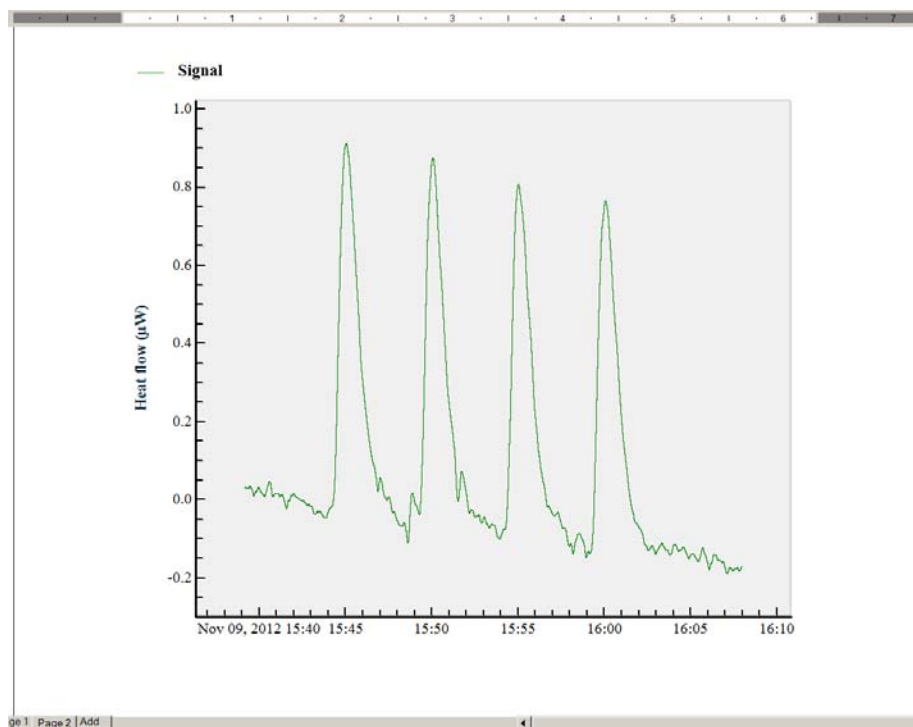


Figure 3.2-2 Heat flow generated by the titration of 10 μL water per aliquot, 4 aliquots total, into a 900 μL water volume.

Heat Flow in Salt

The heat flow of a benchtop piece of salt, i.e. with both surface water and with inclusions visible at 10X via microscopy, was also examined. In the data trace shown in Figure 3.2-3, we observe general heat flow (the sum of the heat capacity of the salt crystal, water and the relative imbalance between the sample and reference hastelloy ampoules) which shows intermittent peaks in the negative direction, i.e. absorption of heat into the reference side. The heat flow provided here is relative, since acquisition times are long and using an empty sample/reference cell reference run to determine absolute heat flows would double the time required. At first glance, one might be tempted to ascribe them to heating behaviors of the brine inclusions (see Figure 3.2-3).

Next, we placed the salt crystal to be analyzed into a drybox atmosphere for approximately one week to remove surface water. The resultant heat flow behavior, verified with multiple runs, is that what heat flow behavior we do see is much broader in nature (see Figure 3.2-4). If the heating of the salt crystal is isothermal, rather than a gradient application as was used in studying the possible migration of inclusions under thermally hot repository conditions, one would generally expect this type of behavior. Overall, it is interesting to note that chemical processes with heat signatures are being observed well below 100 °C and further work is planned to link this signature to specific phase transitions or chemical reactions.

3.2.4 Overall Status and Assessment of Techniques

The gravimetric approach, where large samples of salt (100 g levels) are used and the salt is ground up seemed to give reasonable and reliable results. This is a destructive method and is probably best for benchmarking other techniques. Some further work is needed to develop a more specific procedure and confirm that all of the water content is being detected.

The Karl-Fischer coulometric approach is likely to work but a definitive method is not yet developed. This is the same for the microcalorimetry approach where a number of heat signatures are being observed. Both of these techniques will be destructive and suffer from the limitation of needing relatively small samples (gram level or less) where the heterogeneity of the salt sample will be a significant issue in the overall interpretation of the results. Further work on both of these techniques is ongoing.

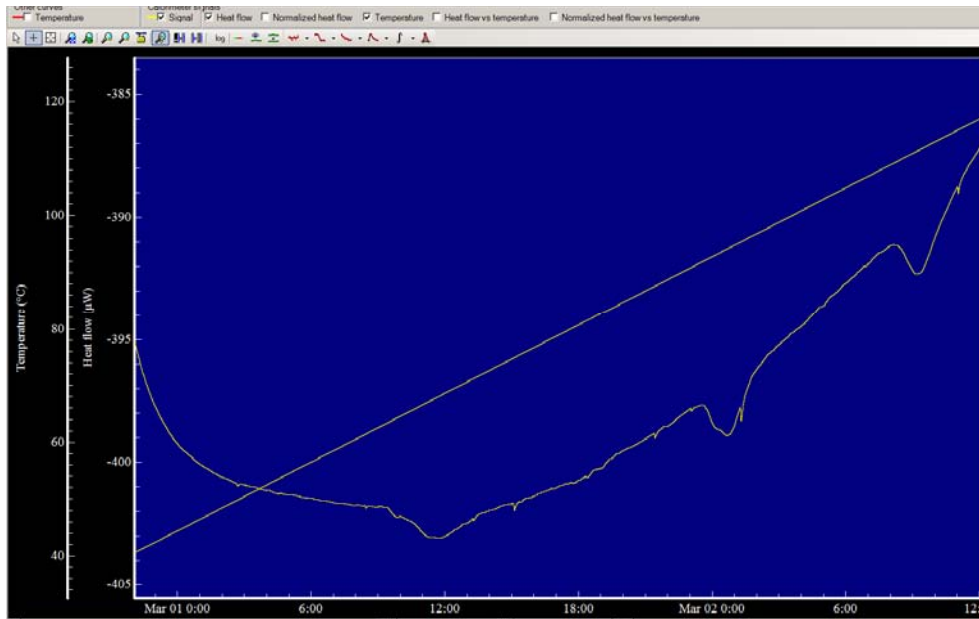


Figure 3.2-3 Relative heat flow over time for benchtop salt crystal. The straight line is the temperature vs. time curve.

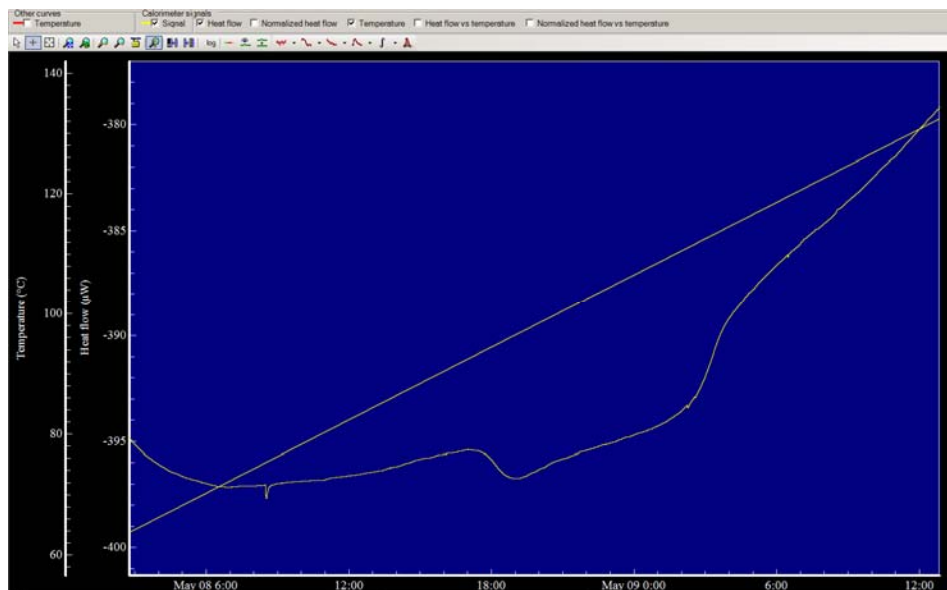


Figure 3.2-4 Relative heat flow over time for thoroughly dried salt crystal. The straight line is the temperature vs. time curve.

4.0 Status of Experimental Results: Biogeochemistry of Neptunium (V)

The status of experimental results on the following three Tasks is reported:

Task 3: Microbial Characterization of Gorleben Salt and Biosorption

Task 4: High Ionic-Strength and Temperature Effects on the Np(V) Aquo species

Task 5: Np(V)-Borate Complexation

4.1 Task 3: Microbial Characterization of Gorleben Salt and Biosorption

Significant progress has been made in the microbial characterization indigenous microorganisms in the WIPP (Swanson et al., 2013, “Microbial Characterization of Halite and Groundwater Samples from the WIPP,” Report LA-UR 13-26280, Los Alamos National Laboratory). Microbial effects remain a key contributor to engineering decisions in the operation of the WIPP repository and an accounting of their possible effects is critically needed for the extension of this salt repository concept to the higher temperatures and different nutrient mix of an HLW/SF thermal repository. At the elevated temperatures and radiation levels, it is expected to show that microbial effects, at least in the near field, are not important.

In this Task, as part of our collaboration with German repository scientist, the microbial characterization work was extended to Gorleben salt. Gorleben is the German site that is currently under consideration for an HLW/SF salt repository.

Samples of halite from Gorleben were analyzed for microbial characterization. Thus far, no *Archaea* and no eukaryotes have been detected from raw halite. These halite samples were inoculated into growth media and analyzed. Low-salt incubations of hydrocarbon-contaminated halite resulted in the growth and isolation of two bacterial species, *Brachybacterium* sp. and a *Yaniella*-like organism (96% similarity in DNA sequence suggests different, but related, genus, currently unclassified). Although neither has been previously shown associated with halite, members of the genus *Yaniella* have been isolated from saline soils and *Brachybacterium* spp. have been isolated from oil brines. Members of both are halotolerant or moderately halophilic. Some *Brachybacterium* spp. are hydrocarbon degraders. High-salt incubation of the hydrocarbon-contaminated halite has yielded growth of *Chromohalobacter* sp. Clones derived

from direct extracts of DNA from raw halite (non-hydrocarbon) match to uncultured *Halanaerobiaceae*. Incubations are still being monitored and have not yet been screened for Archaea.

Specific to the biosorption experiments, *Chromohalobacter* was detected in high-salt incubations of the hydrocarbon halite – so this is a microorganism that is common to both the WIPP and Gorleben. *Brachybacterium* (see Figure 4.1-1) was both detected and isolated from low-salt incubations of the same. The *Halocella*-like sequences (possible cellulose degrader) were detected in the uncontaminated raw halite. An additional organism (*Yaniella* sp; hydrocarbon degrader) was isolated from the low-salt hydrocarbon incubations.

A comparison between what has been observed in the WIPP and the Gorleben environs is shown in Figure 4.1-2. This work continues as part of the NEA salt club activity and a continuing collaboration between LANL researchers and Rossendorf.

An extension of this microbial work is the biosorption of Np(V) towards both archaea and bacteria in high ionic strength systems. We have already published the biosorption of Np(V) onto bacteria (Ams, D. A., J. S. Swanson, J. Szymanowski, J. B. Fein, M. Richmann and D. T. Reed. 2013. *The Effect of High Ionic Strength on Neptunium (V) Adsorption to a halophilic bacterium*. *Geochimica et Cosmochimica Acta*, 110: 45057-45063). Figure 4.1-3 shows the comparative biosorption of Np(V) towards *Halobacter noricense* (an archaea) where much less sorption was observed.

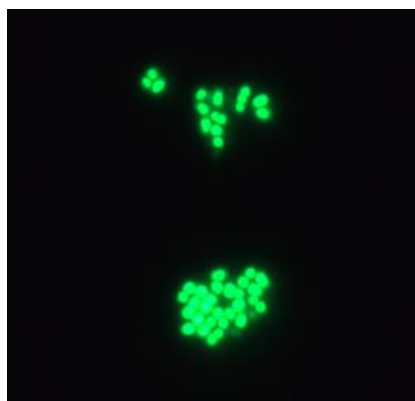


Figure 4.1-1 *Brachybacterium* sp. epifluorescent signature

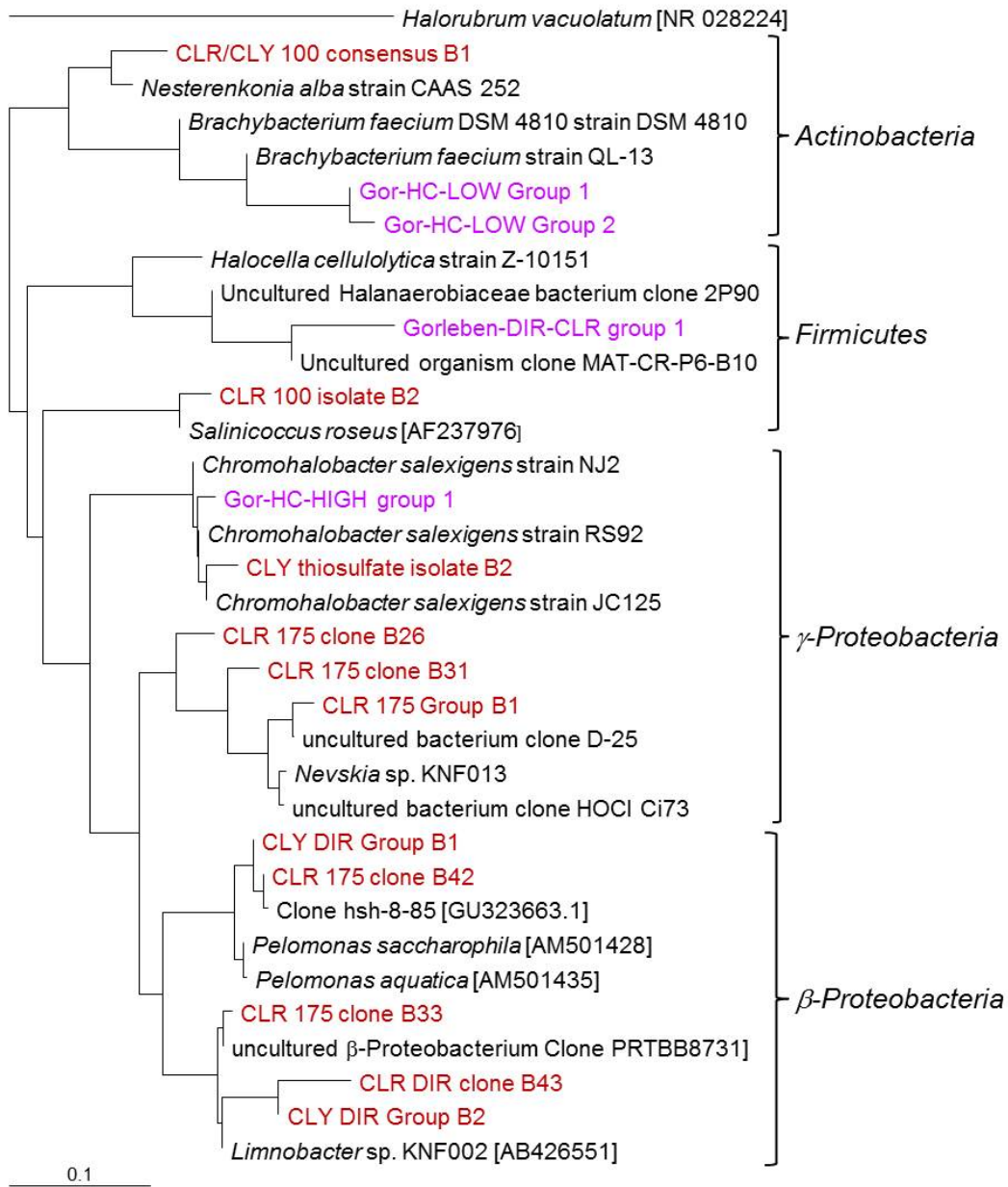


Figure 4.1-2 Phylogenetic tree that compares what has been observed in the WIPP (red) to the Gorleben salt analyses (pink) in progress

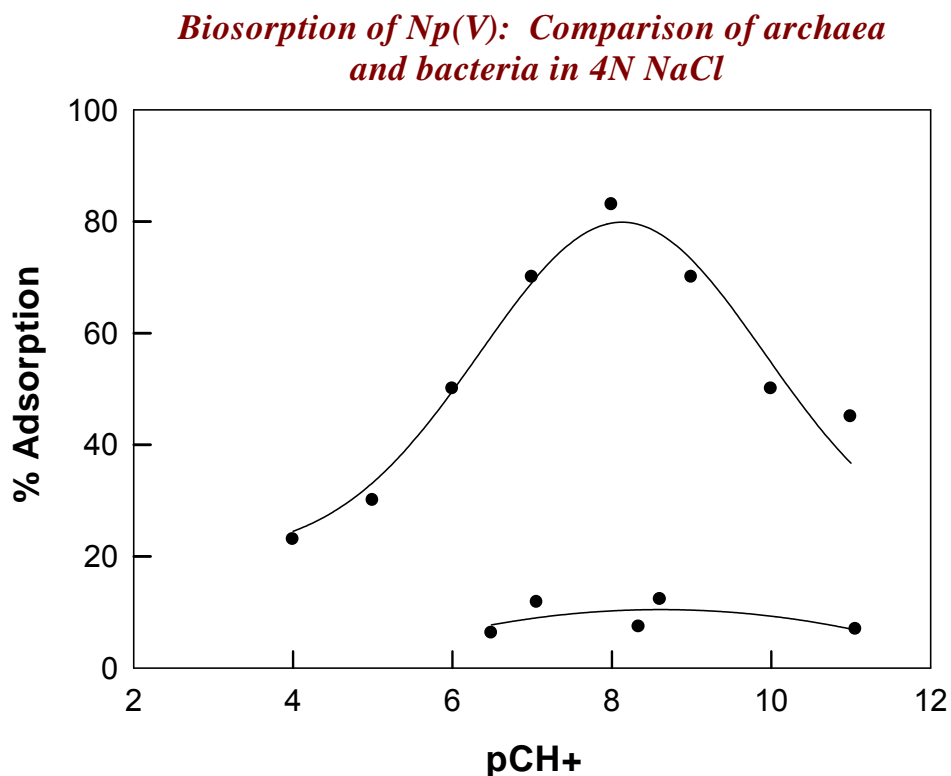


Figure 4.1-3 Comparative biosorption of Np(V) towards *Halobacterium noricense* (bottom curve) and *Chromohalobacter sp.* (top curve). This shows the archaea to be much less sorptive than the bacteria under comparable conditions

4.2 Task 4: High Ionic-Strength and Temperature Effects on the Np(V) Aquo species

The biogeochemistry of neptunium is critical to the long-term assessment of a HLW/SF repository since it tends to be mobile in the subsurface and grown in, with time, due to the natural decay of other key transuranic isotopes. As a first step to evaluating its aqueous chemistry for heated brine systems, the spectroscopy of the aquo species was evaluated as a function of ionic strength and temperature. This is fundamental information that will be coupled with Np phase analysis to establish and evaluate its overall solubility in brine systems at elevated temperature.

4.2.1 Np(V) aquo spectrum as a function of Temperature

Studies were performed to examine the behavior of Np aquo lineshape and position in weak HCl media as a function of temperature. Fitting of the lineshapes at a variety of temperatures showed that the line center wavelength shifted as $f(T)$. Unlike the constant temperature case, the lineshape itself changed as temperature changed, both in terms of width and also the Lorentz/Gauss ratio used in the pseudo-Voigt lineshape function. The results for linewidth vs. temperature, line center vs. temperature and Lorentz/Gauss ratio vs. temperature are shown in Figures 4.2-1, 4.2-2 and 4.2-3 respectively. These changes have been fit/modelled and can be used to adjust for spectra at elevated temperature.

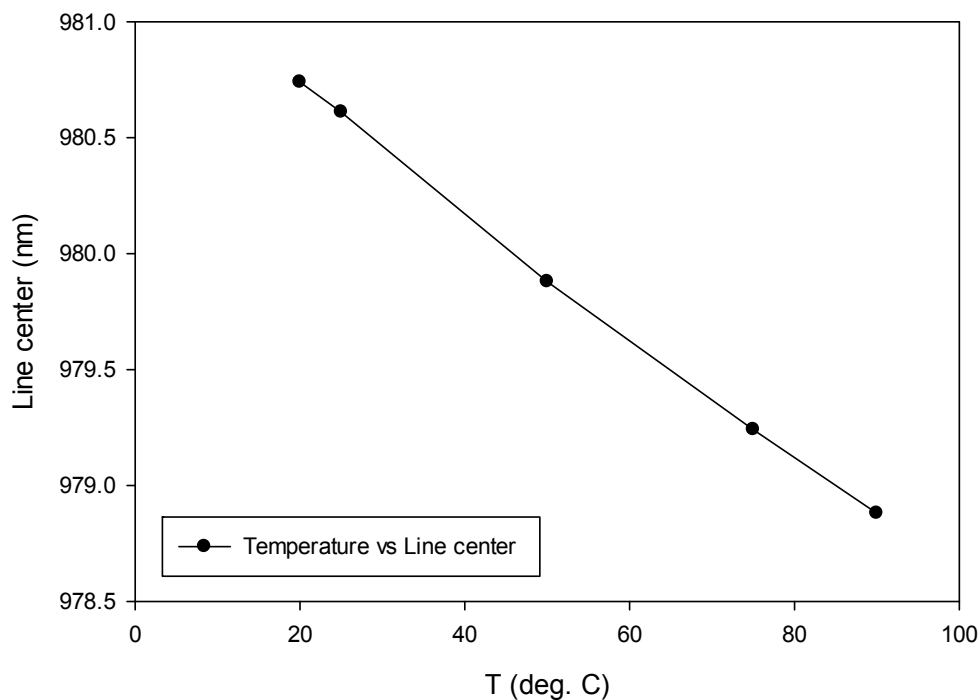


Figure 4.2-1 Np aquo peak line center position as a function of temperature in 0.1 M HCl.

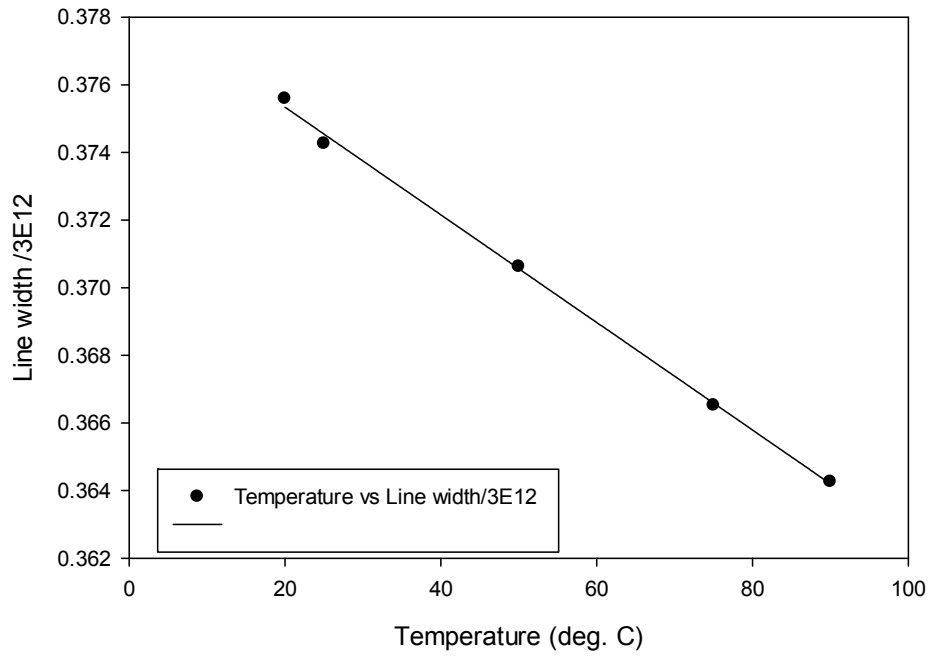


Figure 4.2-2 Np aquo peak width as a function of temperature in 0.1 M HCl.

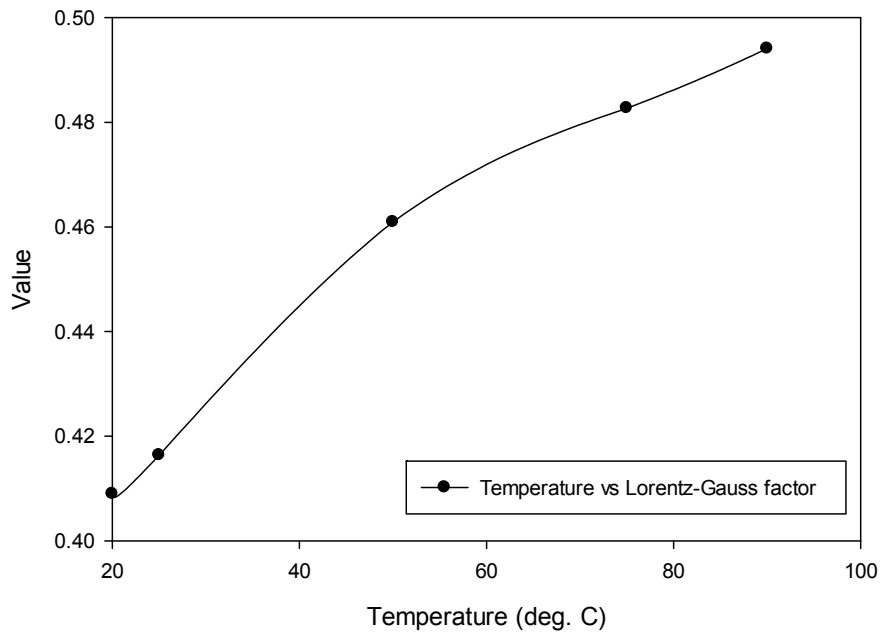


Figure 4.2-3 Np aquo peak Lorentz/Gauss ratio as a function of temperature in 0.1 M HCl.

4.2.2 Np(V) aquo Spectrum as a Function of Ionic Strength

The effects of ionic strength on the Np(V) aquo spectrum was evaluated in sodium perchlorate (non-complexing) and sodium chloride media. As was the case with temperature, a peak shift was noticed at $I > 3$ M and these changes need to be accounted for in speciation studies.

The absorption spectra obtained over the range of 0.1-8.4 M perchlorate was essentially constant in shape (see Figure 4.2-4) but with a peak-center wavelength that varied significantly (blue shift) and smoothly as a function of perchlorate concentration (see Figure 4.2-5).

In sodium chloride, however, a red-shifted peak was noticed (see Figure 4.2-6). This was attributed to complexation by chloride at the highest chloride concentrations and can be interpreted as the sum of the aquo peak (from the perchlorate data) and a peak for the chloride complex formed. The fit coefficients as a function of $[\text{NaCl}]$ is shown in Table 4.2-1. Whether the 3 M case is discordant or represents the true K_{app} vs. $[\text{NaCl}]$ curve is not clear at this point. Discounting it yields a $\log(K_{\text{app}})$ value of ~ -0.8 .

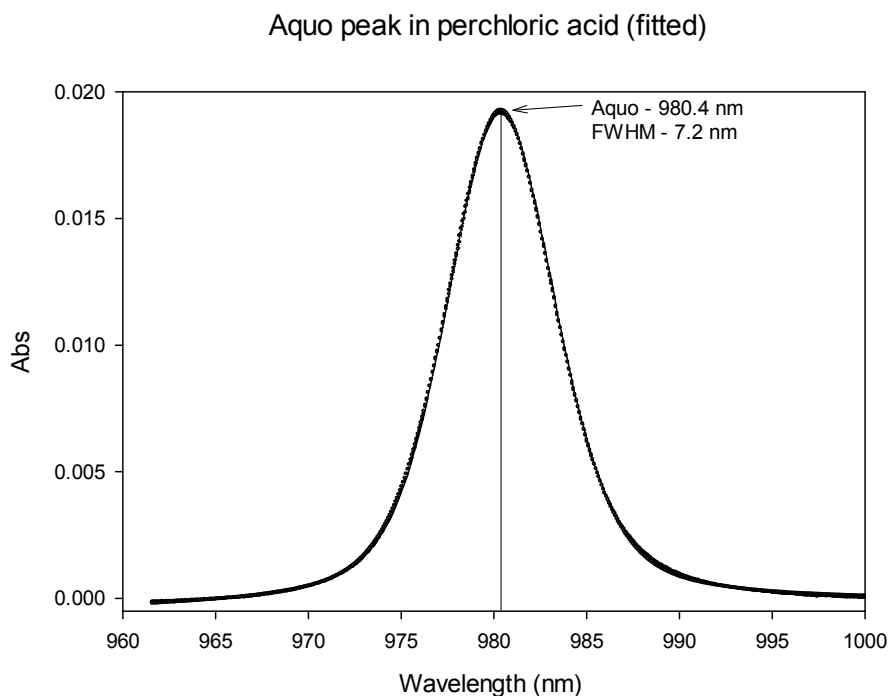


Figure 4.2-4 Aquo Np(V) peak in Perchloric Media

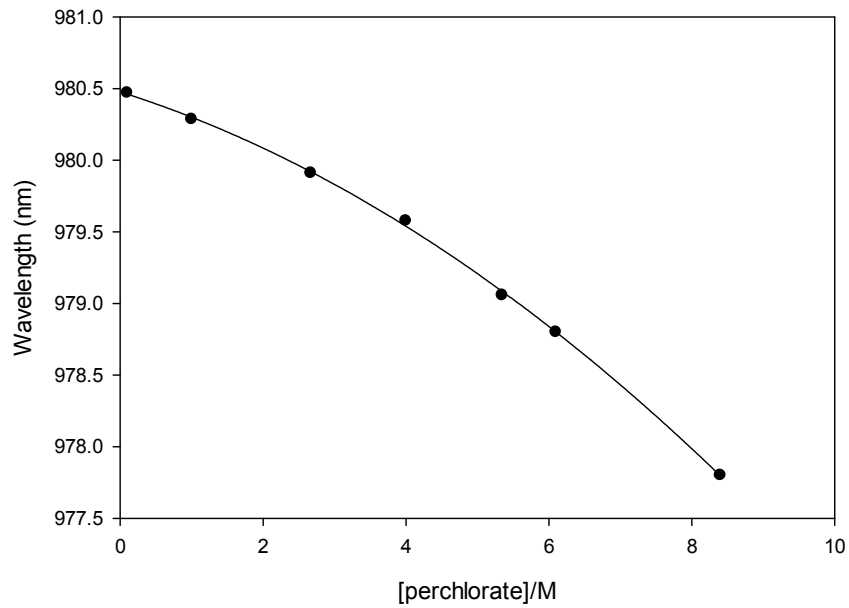


Figure 4.2-5 Variation of Np aquo peak center wavelength as a function of perchlorate concentration at constant temperature.

Np in 5 M NaCl

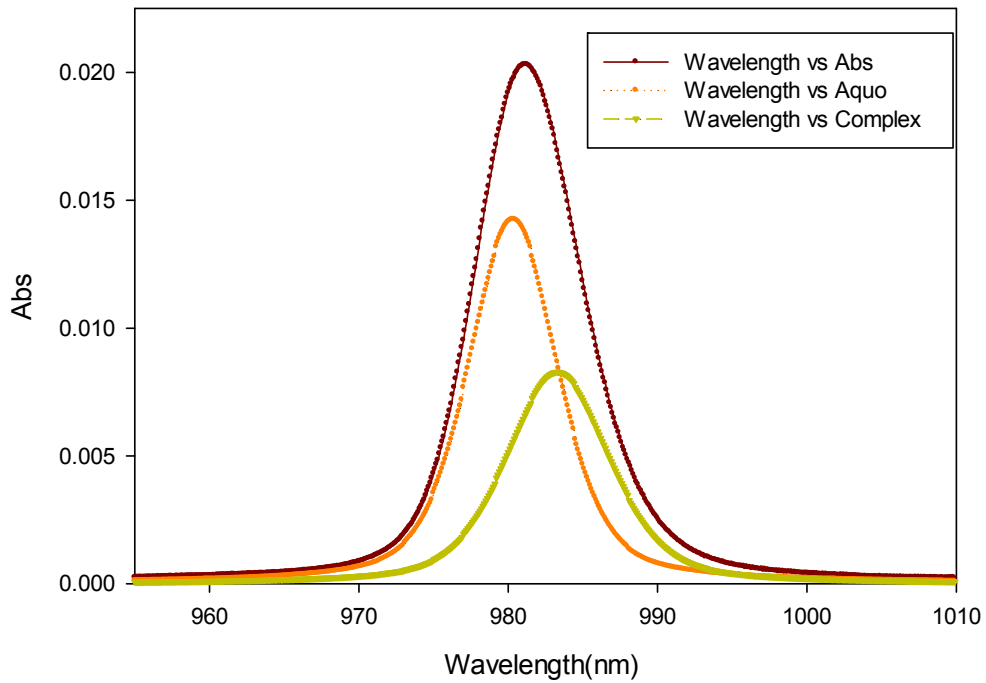


Figure 4.2-6 Np(V)-chloride peak observed at the highest ionic strengths investigated

Table 4.2-1 Fit coefficients for Np(V) in NaCl medium					
[NaCl] (M)	Np chloride peak*1000	Np aquo peak*1000	Np chloride/Np aquo	K_{app}	Log(K_{app})
0.5	1.6871	20.3103	0.0831	0.1661	-0.780
1.0	2.7548	18.9546	0.1453	0.1453	-0.838
3.0	3.9439	16.7571	0.2354	0.0785	-1.105
5.0	9.6070	12.1460	0.7910	0.1582	-0.801

4.3 Task 5: Np(V) Borate Complexation

Borate is ubiquitous in salt and its presence in solution will form a complex with Np(V) that will affect the overall solubility of the neptunium. This complexation is being evaluated and the complex itself, once this has been modeled, will be used in a model study of temperature-variable effects. The results for the 25°C study are summarized in this report.

The formation of a borate complex leads to new band formation and a red-shifted peak at 987 nm (see Figure 4.2-7). This forms an isobestic point, indicating that only a 1:1 borate complex is being formed at variable pH (Figure 4.2-8) and variable borate concentration (Figure 4.2-9).

Fitting coefficients were determined and the calculated apparent complexation constants are shown in Table 4.2-2. The average K_{app} for the set is 2.11±0.08. This value becomes important when compared to other complexation processes that take place in various media, in particular solutions with chloride, which also complexes neptunium but much more weakly so than borate. Overall, the relative peak positions of the aquo, carbonate and borate complexes are summarized in Figure 4.2-10

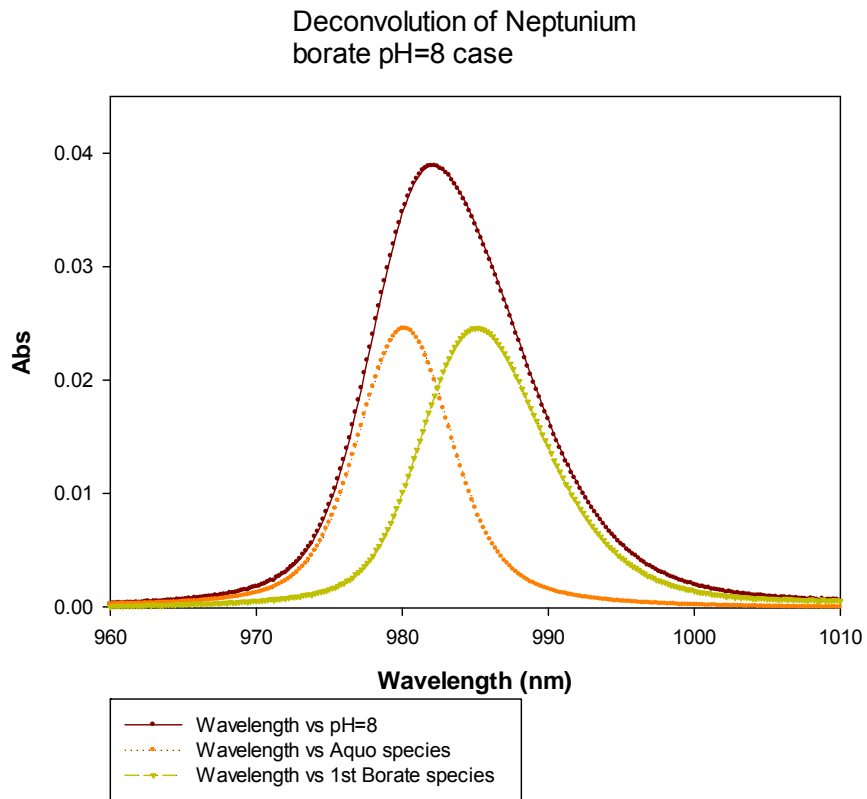


Figure 4.2-7 Deconvolution of the Np(V)-borate complex at pH 8 into the aquo peak (980.2 nm) and the borate complex (987 nm).

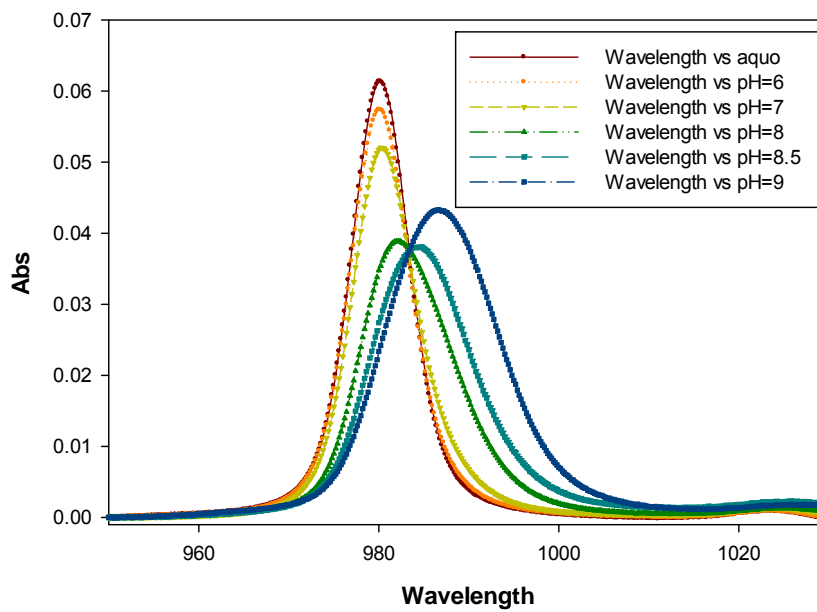


Figure 4.2-8 Isobestic point with Np(V) borate complexation as a function of pH

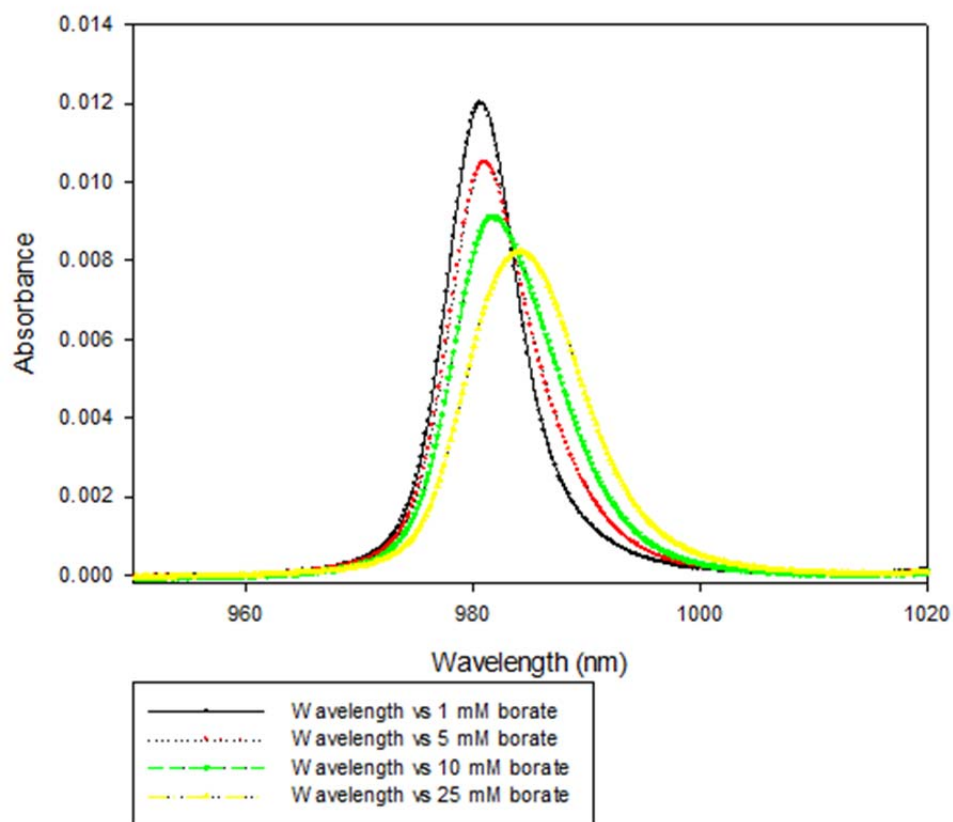


Figure 4.2-9 Spectra for constant [Np] and varying [borate] at nearly constant pH to examine isobestic behavior.

Table 4.2-2 Fitting coefficients and parameters for Np(V) with borate at ~ constant pH						
Borate concentration	pH	Np borate peak*1000	Np aquo peak*1000	Np borate/Np aquo	K_{app}^*	Log K_{app}
1 mM	8.83	1.57	11.4	0.138	138	2.139
5 mM	8.99	3.80	7.81	0.487	97	1.988
10 mM	9.03	5.88	4.37	1.35	135	2.129
25 mM	9.07	7.55	2.03	3.72	149	2.173

*Using total tetraborate concentrations

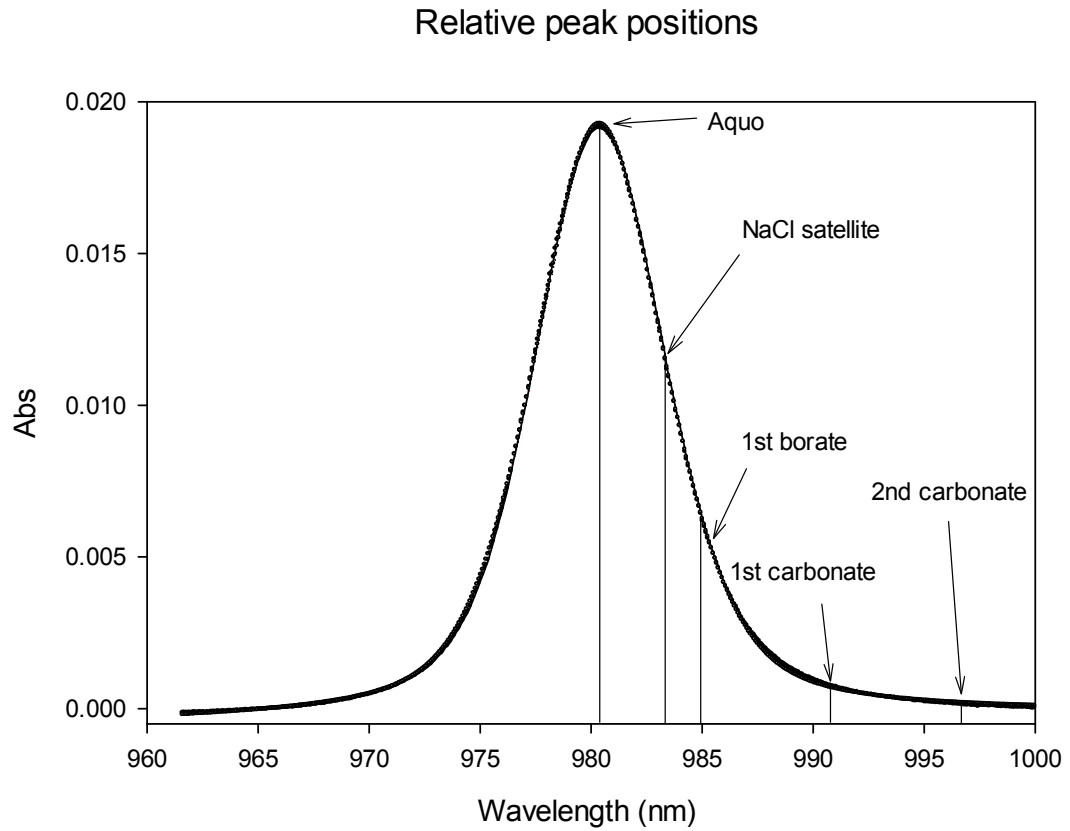


Figure 4.2-10 Relative peak positions of the various complexes in the Np(V) aquo, carbonate and borate system.